

Modification of Heating Profile Sintering cycle Enhance the Physical and Mechanical properties of Sintered Products

Alhadi A. Abosbaia, Stephen Mitchell, and Andrew Wronski

Abstract— A frequent problem associated with steel liquid phase sintering is the occurrence of non-uniform porosity, resulting from gaseous reactions within the compact as the temperature is raised. Such porosity, especially near the component surface, can lead to premature catastrophic failure. This problem was investigated in the ultra-high carbon steel Fe-1.2-1.4C-0.65Si-0.85Mo. An imperfect solution was vacuum sintering, successful for removing CO. During conventional gas sintering, however, gas escape routes are blocked until carbon dissolution starts. The other requirement is the reduction of powder water content-to control initially steam and subsequently CO/CO₂ production. HSC Chemistry 5.11 computer software was used to calculate the partial pressures of O₂, CO, CO₂, CO/CO₂, H₂O, H₂ and H₂/H₂O versus temperature. This enabled a successful solution to porosity problems, when sintering in N₂-10%H₂, by modifying the heating rate profile and the sintering cycle. Uniform densification to above 7.75g cc-3 was attained.

Keywords— liquid phase sintering, gas porosity, heating profile sintering cycle.

I. INTRODUCTION

POWDER Metallurgy ultrahigh carbon steels, UHCSs, have been investigated especially by Sherby et al. [1-4] and latterly by Abosbaia et al [5-7], utilising liquid phase sintering. Alloying elements such as those used in this presented work e.g. Mn, Cr and Si are elements which have high oxygen affinity and tend to produce thermodynamically stable oxides. Oxides, present on powder particles as a very thin layer, obstruct diffusion during sintering and may inhibit the metallic bonding (neck growth) between particles and reduce liquid phase penetration. Consequently, the physical and mechanical properties of the final sintered products can be affected. Therefore, a protective atmosphere with low oxygen partial pressure is required to reduce these oxides [8]. Accordingly, consideration of the appropriate thermochemical reactions (combined action of admixed carbon and oxygen potential of sintering atmosphere) is essential to determine the correct choice of atmosphere for sintering of these ferrous PM alloys [9-10].

Alhadi A. Abosbaia is with the faculty of engineering, Zawia University, Libya, (drabosbaia@zu.edu.ly)

Stephen Mitchell and Andrew Wronski are with the school of engineering, Bradford University.

II. EXPERIMENTAL PROCEDURES

HöganäsAstaloy Mo85HP was used as the base iron powder. 1.2-1.45 wt.% carbon was introduced as fine Grafitwerk UF4 graphite (of 99.5% purity) and silicon was added as fine <9 µm silicon carbide powder-Turbula powder mixing was performed as follows: the base and silicon carbide powders were dry mixed for 20 minutes. Then 0.5 cc of polypropylene glycol, diluted to 50% by methanol, was carefully added to 100 g of powder and mixing resumed for 20 minutes - in order to coat the metal powders with polypropylene glycol. The mixing was then stopped, graphite powder added and mixing re-started in order to 'glue' the graphite to the base powder particles green specimens (compacts pressed at 500 to 700MPa) of size ~15.3×15.3×4 mm³ were sintered under both vacuum (~10-6 mbar) and dried Nitrogen/Hydrogen (10N₂-H₂)gas (< -60°Cdewpoint to meet the required specification without any oxidation).

Initially heating rates were 10°C -min-1 to 600°C with a hold of 30 minutes for the removal of lubricant and adsorbed water and hydroxides, then 10°C min-1 to 900°C, with a hold of 2 hours, to allow distribution of carbon and silicon, followed by heating to the sintering temperature at 5°C/min, with sintering time of 30-60 minutes at temperatures varying from 1285 to 1300°C. After sintering, the specimens were allowed to cool slowly to room temperature. This heating cycle produced a non-uniform microstructure with large connected pores. It was obvious that the large porosity observed was the result of evolved gas pressure, therefore different heating profiles were studied to try to minimise CO/CO₂ evolution and concurrently take graphite into solution as quickly as possible to create sufficient interconnected porosity to relieve any build up of gas pressure. Modifying the heating profile cycle was required in order to obtain uniform microstructure with best densification.

Figure 1 and Table 1, show different microstructures produced by processing in different heating cycle profiles for the same composition. The first heating cycle was heating to 600°C for 15 min with heating rate 10°C -min-1, followed by heating to 1100°C for 20 min, then furnace cooling. Second heating cycle was to heat the samples to 730°C for 15min, with heating rate 10°C -min-1 followed by heating to 1100°C for 20 min, then furnace cooling. Third heating cycle was by heating straightaway to 750°C for 15 min with heating rate 10°C -min-1, followed by heating to 1100°C for 20 min, then furnace cooling. Fourth heating cycle was by heating

straightaway to 900°C for 15 min with heating rate 10°C - min-1, followed by heating to 1100°C for 20 min, then furnace cooling.

III. RESULT

Microstructural observations of initially sintered specimens showed excessive porosity. Examination of microstructures such as those of Figures 2 led to the belief that the additional porosity and its size must be linked to gas evolution during the heating cycle.

It was obvious that some gas ‘bubbles’ were still preventing maximum densification during sintering. It was therefore decided to adjust the conventional sintering heating profile to minimise the amount of alpha sintering due to the Fe in Fe self diffusion by speeding up the heating rate and also increasing the temperature for the first hold to above the alpha-gamma transition temperature. Figure 3, reveals that the fourth heating cycle profile shows least gas porosity and better uniform microstructure (higher density ~7.75g/cm³ as listed in Table 1) with very tiny pores.

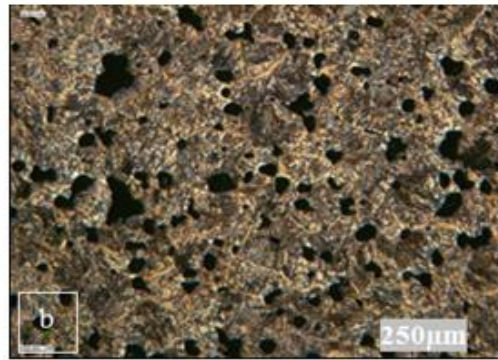


Fig. 2 Microstructures of Fe-0.85Mo+0.6Si+1.4C(+0.5cc liquid paraffin), sintered at 1300°C for one hour in, 90N₂/10H₂ gas using initial cycle

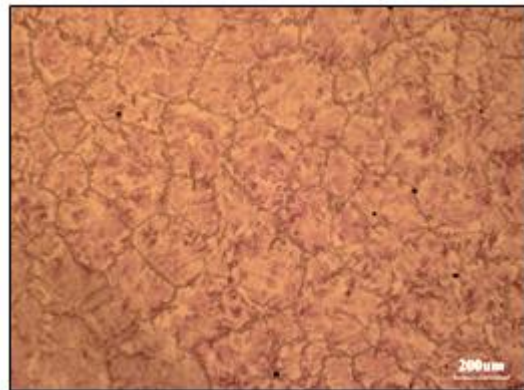


Fig. 3 Microstructures of Fe-0.85Mo+0.6Si+1.4C (+0.5cc liquid paraffin), sintered at 1300°C for one hour in, gas atmosphere (90N₂/10H₂), using fourth heating cycle.



Fig. 1 Different microstructures for the same alloy composition Fe-0.85Mo+0.6Si+1.4C processed by different heating cycle profiles, a) First heating cycle, b) second heating cycle, c) third heating cycle and d) fourth heating cycle.

TABLE 1
SHOWS THE TYPES OF HEATING SINTERING PROFILE USED IN THIS WORK

Sintering Cycles	R _{m1}	Lubricant Burn-off		R _{m2}	Carbon Diffusion		R _{m3}	Homogenization		R _{m4}	Sintering		Sintering Density (g/cm ³)
		T	t		T	t		T	t		T	t	
Cycle 1	5	450	15	10	600	30	10	900	120	5	1285-1300	30-60	7.15 - 7.27
Cycle 2	5	450	15	10	730	30	10	900	120	5	1285-1300	30-60	7.25 - 7.32
Cycle 3	5	450	15	10	730	30	10	900	120	5	1285-1300	30-60	7.31 - 7.45
Cycle 4	5	450	15	20	900	15	10	1100	120	5	1285-1300	30-60	7.42 - 7.75
GA	Pure N ₂			(90N ₂ /H ₂)									
R _m -Ramp (°C/min) T-Temperature (°C) t-Time (min) GA- Gas Atmosphere													

IV. DISCUSSION

Thermocalc predicted the necessary compositions and sintering temperatures to produce sufficient liquid phase for densification of these ultra-high carbon steels. Accordingly, processing was performed but, despite some densification, the microstructure contained large pores and consisted of pearlite plus thick, brittle cementite networks.

Therefore, HSC chemistry software was used to model the possible gas reactions, e.g. $C + H_2O \rightarrow CO_2 + H_2$, water-gas shift reaction: From $\sim 500^\circ C$, $C + 2FeO \rightarrow 2Fe + CO_2$ found to be favourable from $\sim 500^\circ C$, and $C + CO_2 \rightarrow 2CO$ Boudouard reaction: From $\sim 500^\circ C$ complete $\sim 930^\circ C$.

These findings led to belief that water must be adsorbed onto the surface of the powders, particularly graphite with its large specific surface. Therefore, powders were dried in a vacuum oven, mixed and sintered. The results were much improved but still showed some significant porosity and again thick, cementite networks

From Figure 4, it easy to see graphite and silicon blocking porosity at $600^\circ C$ and preventing gases from escaping. Figure 5 shows that the graphite has just started to react but not completely, whereas the silicon has not begun to react yet even in the austenitic region at temperature of $\sim 750^\circ C$, thus the network of grain boundaries were still semi blocked. Figure 6 shows that the graphite and silicon were already starting to diffuse into austenite at $900^\circ C$, as the temperature increases further more diffusion takes place, which leads to more uniform contact melting, faster neck growth between particles and higher amount of liquid phase formation, before furnace cooling.

When the sintering cycle was modified to minimise the amount of alpha phase sintering and to release gases from pores by speeding the heating rate to $20^\circ C/min$, reducing the time of the $900^\circ C$ hold to 15 mins, but increasing the temperature of the diffusional/homogenisation hold to $1100^\circ C$, a network of grain boundary pores formed, allowing penetration of a liquid phase as it formed at the sintering temperature, thus producing higher densification.

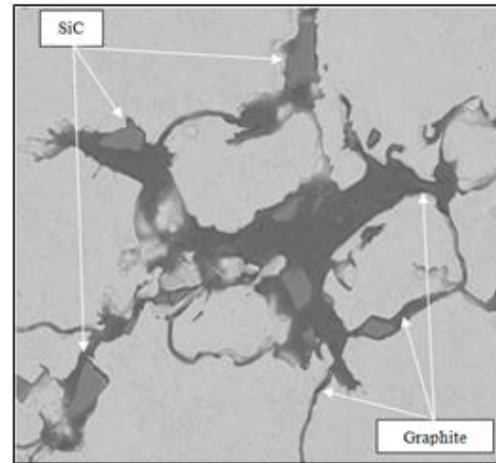


Fig. 4 Scanning electron micrograph of microstructure of Fe-0.85Mo+1.4C+0.6Si, heated to $600^\circ C$ for 15min with heating rate $10^\circ C \cdot min^{-1}$, and followed by furnace cooling.

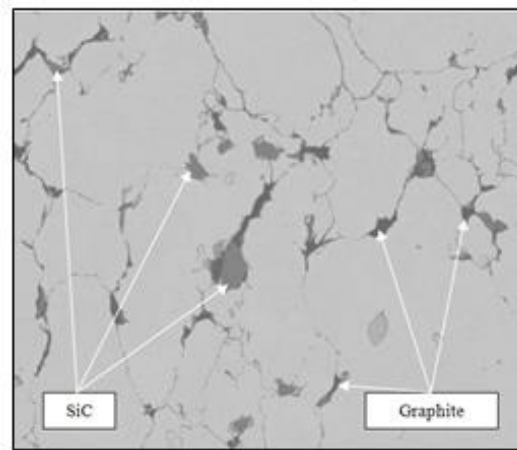


Fig. 5 Scanning electron micrograph of microstructure of Fe-0.85Mo+1.4C+0.6Si, heated to $750^\circ C$ for 15min with heating rate $10^\circ C \cdot min^{-1}$, and followed by furnace cooling.

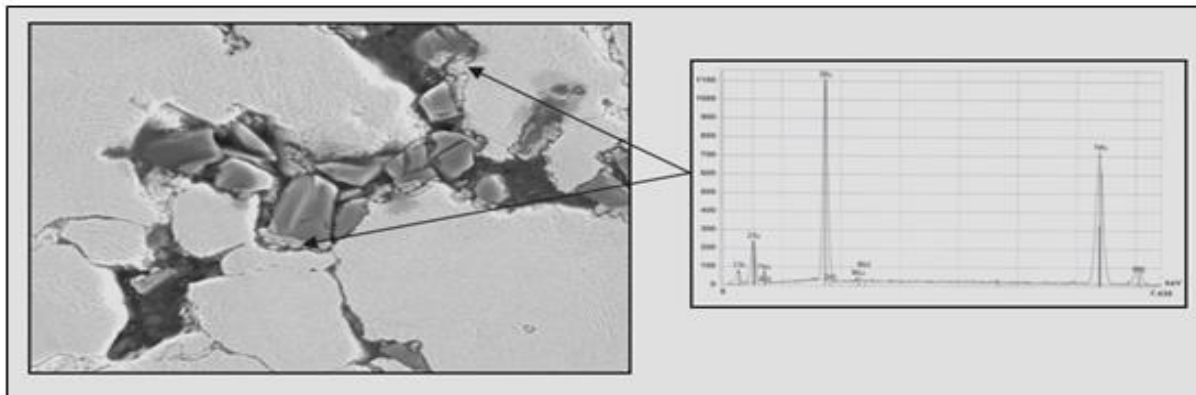


Fig. 6 Scanning electron micrograph of microstructure of Fe-0.85Mo+1.4C+0.6Si, heated to $900^\circ C$ for 15min, with heating rate $10^\circ C \cdot min^{-1}$, and followed by furnace cooling. Pearlite is now in evidence as graphite diffusion has taken place

The 90N2/10H2 route allows early reduction of the oxidised iron surfaces, which is necessary for graphite to be taken into solution as austenite forms [9]. When graphite is taken into solution, paths appear between powder particles to allow escape of CO/CO₂, thus preventing build up of potentially damaging gas pressure.

IV. CONCLUSION

Predicted data obtained from Thermo-Calc software was very much in accord with experimental results. Modifying the heating profile, again industrially attainable, overcomes the problems of large gas porosity and results in uniform high density sintered specimens, i.e. the fourth heating profile used in presented work, produced the best results.

REFERENCES

- [1] Sherby, OD., Walser, B., Young, CM., Cady, EM.: Scripta Met., volo. 9, 1975, p. 569.
- [2] Sherby, OD., Carsi, M., Kim, WJ., Lesuer, RD., Ruano, OA., Syn, CK., Taleff, EM., Wadsworth, J.: Materials Science Forum, vol. 426-432, 2003, p. 11.
- [3] Lesuer, DR., Syn, CK., Whittenberger, JD., Sherby, OD.: Met. Mat. Trans. A, vol. 30, 1996, p.1559.
<http://dx.doi.org/10.1007/s11661-999-0093-x>
- [4] Syn, CK., Lesuer, DR., Sherby, OD.: Met. Mat. Trans. A, vol. 25, 1994, p. 1481.
<http://dx.doi.org/10.1007/BF02665480>
- [5] Abosbaia, AAS.: Ph. D. thesis. University of Bradford, 2010.
- [6] Abosbaia, AAS., Mitchell, SC., Youseffi, M., Wronski, AS.: accepted by Powder Met.
- [7] Szczepanik, S., Mitchell, SC., Abosbaia, AAS., Wronski, AS.: Powder Metallurgy Progress, vol. 10, 2010, p. 59.
- [8] M. Hrubovčáková and E. Dudrová, Thermodynamic and experimental study of role of temperature and graphite additions on oxide reduction during sintering astaloyCrL, ActaMetallurgicaSlovaca, 2009, 15, No. 4: pp. 248-254.
- [9] S. C. Mitchell, A. Cias, Carbothermic reduction of oxides during nitrogen sintering of manganese and chromium steels, Powder Metallurgy Progress, 2004, 4, No. 3: pp. 132-142.
- [10] P. Ortiz and F. Castro, Thermodynamic and experimental study of role of sintering atmospheres and graphite additions on oxide reduction in AstaloyCrM powder compacts, Powder Metallurgy, 2004, 47(3): pp. 291-298.
<http://dx.doi.org/10.1179/003258904225020747>